Journal of ELECTRONIC MATERIALS, Vol. 38, No. 2, 2009
DOI: 10.1007/s11664-008-0590-5
© 2008 TMS
Special Issue Paper

Wetting Kinetics of Eutectic Lead and Lead-Free Solders: Spreading over the Cu Surface

HUI ZHAO,[1] DINESH REDDY NALAGATLA,[1,2] and DUSAN P. SEKULIC[1,2,3]

1.—Center for Manufacturing, University of Kentucky, Lexington, KY 40506, USA. 2.—Department of Mechanical Engineering, University of Kentucky, Lexington, KY 40506, USA. 3.—e-mail: sekulicd@engr.uky.edu

Wetting kinetics of Sn, eutectic Sn-Ag, eutectic Sn-Cu, and eutectic Pb-Sn was studied using real-time *in situ* monitoring of the triple-line movement, facilitated by a hot-stage microscopy system under a controlled atmosphere. Significantly different kinetics of lead versus lead-free solders is documented. In case of the eutectic lead solder, four characteristic spreading stages were identified. Spreading of lead-free solders features two stages with a sharp change of the spreading rate at the early stages of rather insignificant spreading. Scanning electron microscopy and energy-dispersive x-ray spectroscopy analysis of the resolidified solder surface within a halo region is discussed.

Key words: Soldering, lead-free and lead solders, wetting

INTRODUCTION

Soldering technology is extensively used in electronic packaging for consumer products, space, and defense applications.[1] Because lead-free solders impose many practical challenges, sustained research and development in this area is of great importance.[2] The lack of understanding of the mechanism of wetting of molten metal on a substrate during the spreading process hinders continuing efforts to find effective replacements for lead solders.[3] Comparative studies of lead and lead-free solders may offer a needed insight. It is well known that solder systems exhibit significant reactive behavior at the solder–substrate interface.[4] When Sn-rich solders are in contact with a Cu substrate, interface reactions occur and intermetallic compounds (IMCs) Cu_6Sn_5 or Cu_3Sn are formed.[4] A number of efforts have been devoted to the study of wetting kinetics of solder systems.[5–10] Among these, the studies of wettability of lead-free solders, including Sn, Sn-Ag, Sn-Cu, and Sn0.7 Cu-*x*Zn, on Cu substrates by using a wetting balance technique have been reported[8–10]; for example, based on the calculated equilibrium contact angle between molten solder and substrate, it was concluded that wetting of lead-free solders is indisputably inferior to that of Sn-37Pb solder.[8,9] Furthermore, it was demonstrated that the addition of a small amount of an alloying element, such as Zn, to a lead-free solder can change wetting properties, although the change was not significant.[10] Due to the reactive nature of the solder spreading process, it is important to understand how the interface reaction influences wetting. The reaction at the liquid–solid interface (including base metal dissolution and intermetallic compound formation) plays an important role, sometimes even dominating the wetting kinetics. Accordingly, further studies have been devoted to modeling of IMC growth processes.[11] Solder spreading on IMC surfaces with different morphologies was also experimentally studied.[12] Still, the current understanding of wetting processes remains, to a large extent, at a phenomenological level. In-depth analysis of the triple-line kinetics and its dependence on driving and/or retarding forces, including the interplay between capillary forces and interface reactions, is

(Received April 14, 2008; accepted October 3, 2008; published online November 6, 2008)

lacking. The objective of this paper is to offer a contribution to understanding the main kinetic features of molten lead and lead-free solder spreading on Cu substrates. Experimental data on spreading kinetics presented in this paper, including a new set of data for lead-free solders, are complementary to the results presented in Ref. 8.

MATERIALS AND EXPERIMENTAL PROCEDURES

A Linkam THMS 600 hot stage installed on an Olympus BX51M optical microscope system was used for the experimental study (Fig. 1). The working chamber was supplied with ultra high-purity nitrogen (99.999%). A silver block stage, which served as a heater/cooler, delivered heating/cooling by conduction to a base plate (Joule heating or liquid nitrogen, LN2 cooling), with temperature stability better than 0.1 K. The actual temperature of the liquid solder was slightly lower than the temperature reading from the control unit due to thermal contact resistance between the heating element and the sample. This temperature difference (~5°C), which constituted the established experimental bias correction, was registered by monitoring the range of filler metal melting temperatures *in situ* versus the known values for these phase transitions. A substrate coupon having overall dimensions of 10 mm × 10 mm × 0.5 mm was positioned in the chamber over the silver block. The substrate surface finish was not modified (high-purity Cu 122, used as is). Commercial lead and lead-free bulk solder was rolled to a 0.05-mm-thick sheet. Rectangular, approximately square, specimens with dimensions of ~0.5 mm × 0.5 mm were cut from the sheet for the series of hot-stage tests. In each test a solder piece was positioned on the substrate and covered with a fixed amount of rosin-based mildly activated (RMA) flux (EC-19S-8). Solder materials used in this study are listed in Table I. The hot-stage chamber was purged with nitrogen for 120 min before initiation of the heating cycle, which consisted of a ramp up, dwell, and quench. The heating ramp-up was 100°C/min followed by the cooling ramp down of 80°C/min. The digital imaging capture speed was 22 frames/s.

Table I. Lead and Lead-Free Solders Used in Hot-Stage Tests and the Experimental Conditions

Solder Alloy	Melting Temperature (°C)	Peak Temperature (°C)	Dwell Time (s)
Sn-37wt.%Pb	183	213	30
Sn	232	262	10
Sn-0.7wt.%Cu	227	257	10
Sn-3.5wt.%Ag	221	251	10

RESULTS AND DISCUSSION

Figure 2a presents a sequence of instantaneous frames extracted from a digital video clip, illustrating the topology and the location of the triple line throughout Sn-37Pb solder spreading on a copper surface; Fig. 2b and c gives the equivalent spreading radius versus time relation in the form of a linear and a logarithm plot, respectively, for three tests performed under the same experimental conditions. The temperature history imposed is described in Table I. It is clear from the logarithm plot (Fig. 2c) that the kinetics of the spreading process features at least four distinguishable stages, marked as stages I–IV in Fig. 2b and c. At the very beginning of the wetting process, which also involves the solder phase change from a solid to a liquid state, the triple-line location distance [$R = f(t)$] undergoes a very fast (but not necessarily large) increase, i.e., within a very short period of time. The second stage shows a hesitation in the triple-line movement. Subsequently, the spreading slows down (indicated by a smaller slope of the R versus t curve). This relatively short-lived stage was followed by faster spreading until the triple-line movement approached an asymptotic trend. It is worth mentioning that the wetting kinetics illustrated in Fig. 2c resembles the wetting kinetics of a silicon oil drop spreading on a rough glass surface obtained by Cazabat and Cohen Stuart.[13] This similarity may indicate the impact of surface topography at the liquid–solid interface.

After the fast spreading of the molten solder in a short period of time (during stage I), a halo appears

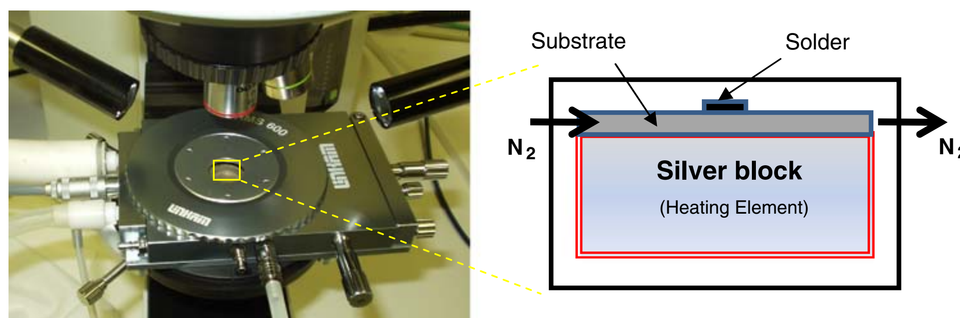

Fig. 1. The experimental setup (a sessile drop sample is positioned within the chamber of the hot stage).

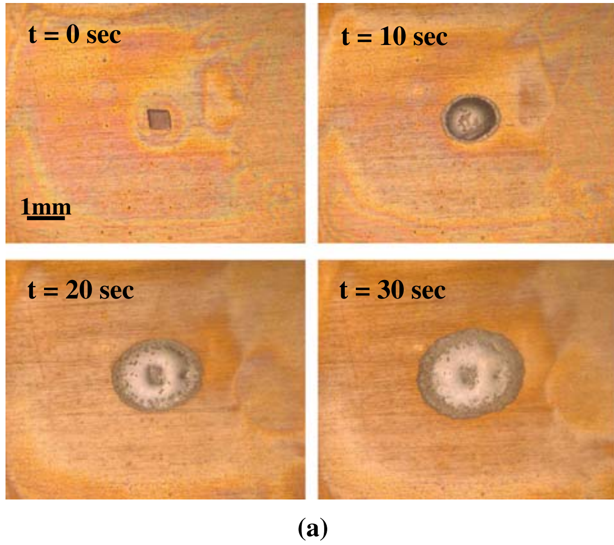

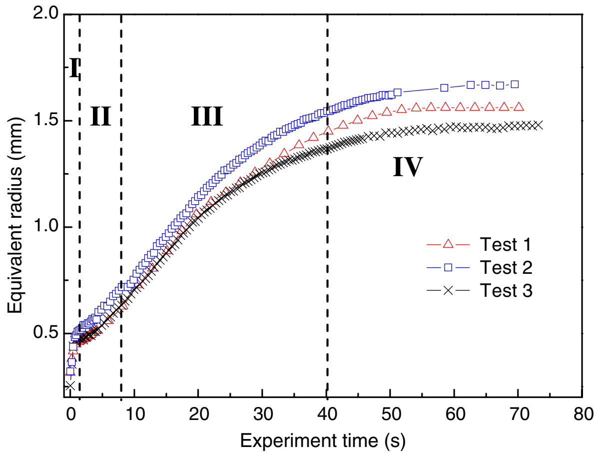

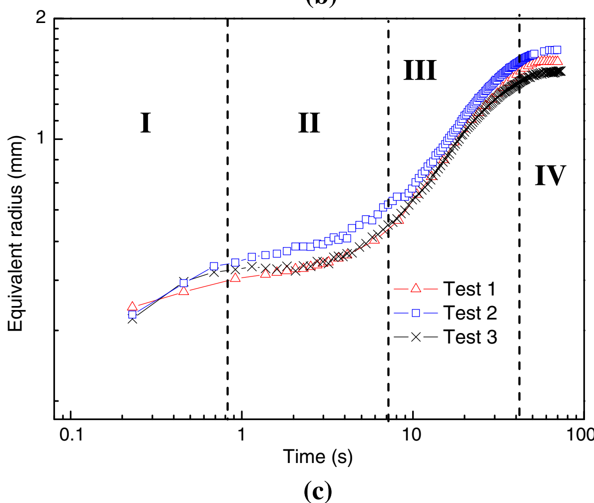

Fig. 2. (a) A sequence of instantaneous frames during eutectic Sn-37Pb solder spreading on a copper surface; (b, c) the correlation between the equivalent radius (R) and time (t).

at the liquid front, moving in front of the edge of the bulk liquid and clearly displaying a circular disc configuration. The width of this halo increases with the movement of the triple line. The configuration of

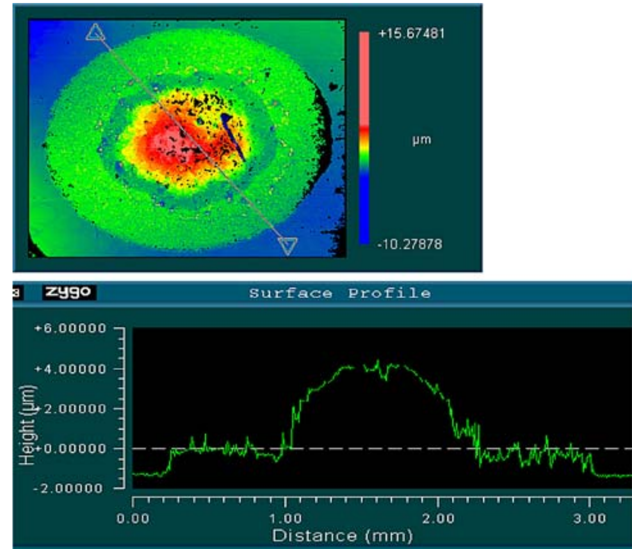

Fig. 3. Surface topography of a resolidified Sn-37Pb solder after hot-stage testing.

the molten solder spread at this stage resembles a "hat with rim" geometry. The surface roughness scan of the resolidified solder shows such a feature in the topographic configuration (Fig. 3). Scanning electron microscopy (SEM) images of the resolidified solder surface are presented in Fig. 4. The existence of the halo is illustrated in Fig. 4a, where the halo is marked as the domain between A and B. Between the halo region and the bulk solder region C, there exists an intermediate zone B, the unique microtopography of which features a distribution of dark-colored islands surrounded by a continuous white phase (Fig. 4c, inset B from Fig. 4a). Energy-dispersive x-ray spectroscopy (EDS) analysis shows that the dominant element in the white phase covering the halo region A is Pb (Fig. 4b, inset A from Fig. 4a). The large amount of Pb appearing in this region might be considered as the residue from a reaction between the liquid solder and the substrate. When a thin layer of solder liquid at the wetting triple line reacts with the Cu substrate, a portion of Sn in the liquid may quickly be exhausted due to the formation of an intermetallic layer. In region B (Fig. 4c) the rough features (the dark-colored islands) contain both Cu and Sn, indicating that this region is a part of the intermetallic layer being exposed. The white-colored phase around these islands contains mainly Pb. Region C (Fig. 4d) is composed of two-phase domains, distinguished by white- and dark-colored features, and characterized by rich contents of Pb, and Sn, respectively. On the other hand, the appearance of a Pb-rich "side band" around the edge of the resolidified Pb-Sn solder on a Cu substrate was reported by Liu et al.[14] However, the width of the "side band" observed in that work was on the microscale and can only be identified under large magnification using SEM. The reported appearance of the microtopography of this outer

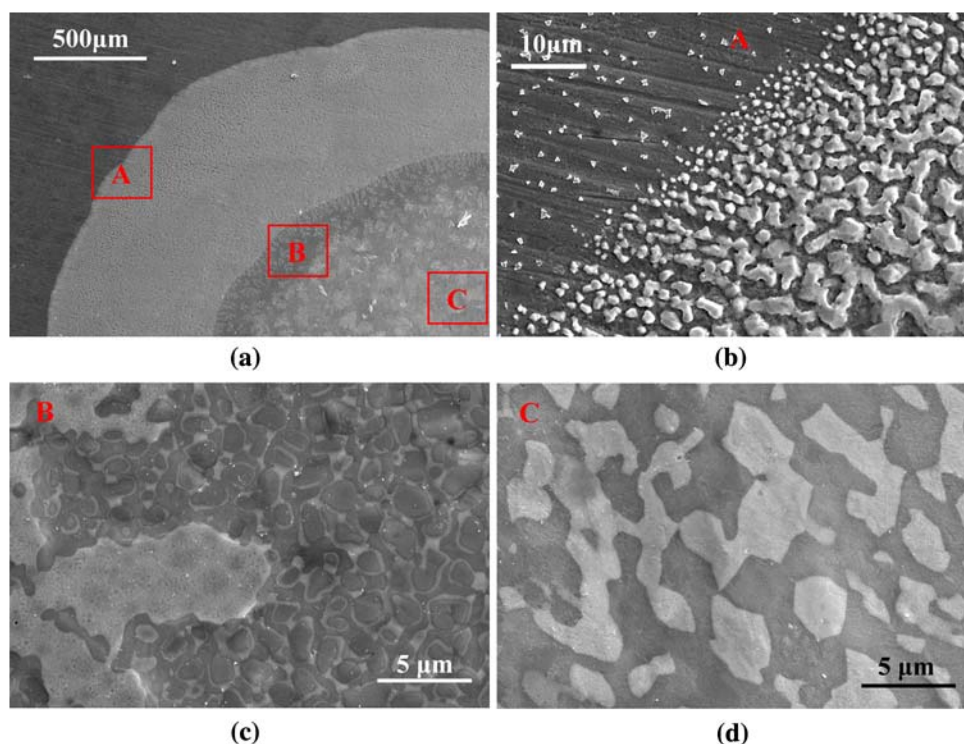

Fig. 4. SEM images of resolidified Sn-37Pb solder surface on a Cu substrate: (a) SEM image under low magnification; (b) SEM image of the halo region A; (c) SEM image of the intermediate region B between the halo and the bulk solder; (d) SEM image of the resolidified solder surface at a central location C.

layer appears quite different from what was observed in Fig. 4b.

Such a configuration of surface microtopography distribution appearance following spreading may offer a hint about the mechanism of wetting behavior of this solder system. Different stages in the evolution of the triple-line location may be related to the appearance of the halo and the intermetallic formation. For example, the initial brief but rapid spreading may indicate that the wetting system is behaving like an inert system; it appears as if the reaction at the interface is not yet sufficiently intensive to influence the triple-line movement. The instant of time when the halo starts to appear at the droplet edge corresponds to the transition from a fast spreading to a relatively slow spreading stage, hence indicating a reaction at the interface that starts to interfere with the wetting kinetics, and eventually becomes the factor controlling spreading. It is not clear what causes the hesitation between the first and third stages of spreading thus structured. This phenomenon may be related to the formation of an intermetallic layer.

Figure 5 offers a set of images of a series of lead-free solder specimens before and after the onset of melting. All lead-free solders considered in this study behave similarly. In all cases solders barely spread over Cu substrates. Figure 6a gives a comparison of the average ratio of the final spreading area versus the initial solder area for all the solders studied. Note that the values of $A_{\mathrm{final}}/A_{\mathrm{initial}}$ for lead-free solders is consistently in the range of 1.2 to 1.4, with Sn-3.5Ag solder showing slightly better wettability than the other two lead-free solders. This consistency may be interpreted as verification of the idea that there is no significant spreading of these lead-free solders. Spreading of lead-free solders shows two stages with a sharp change in the spreading rate, as illustrated in Fig. 6b. Obviously, the large ratio of $A_{\mathrm{final}}/A_{\mathrm{initial}}$ for a eutectic lead solder on a Cu substrate indicates significantly better wetting than for lead-free solders.

After the hot-stage tests, resolidified lead-free solders were examined by using higher-magnification optical microscopy. The appearance of a halo region around the bulk solder was also observed for the lead-free solders (Fig. 7). Because the width of this outer layer is on a microscale, it was not clearly identified during the real-time monitoring of the triple line movement. An *in situ* observation of the halo layer formation using high magnification will be reported elsewhere. SEM images of the halo region of resolidified lead-free solders are presented in Fig. 8. The EDS analysis of this halo region shows the presence of both Cu and Sn. It can be hypothesized that the formation of this layer is closely related to an interface reaction and to the formation of an intermetallic layer.

According to Young's equation, $\cos\theta = (\sigma_{\mathrm{SV}} - \sigma_{\mathrm{SL}})/\sigma_{\mathrm{LV}}$, an increase of either σ_{SL}, the surface tension

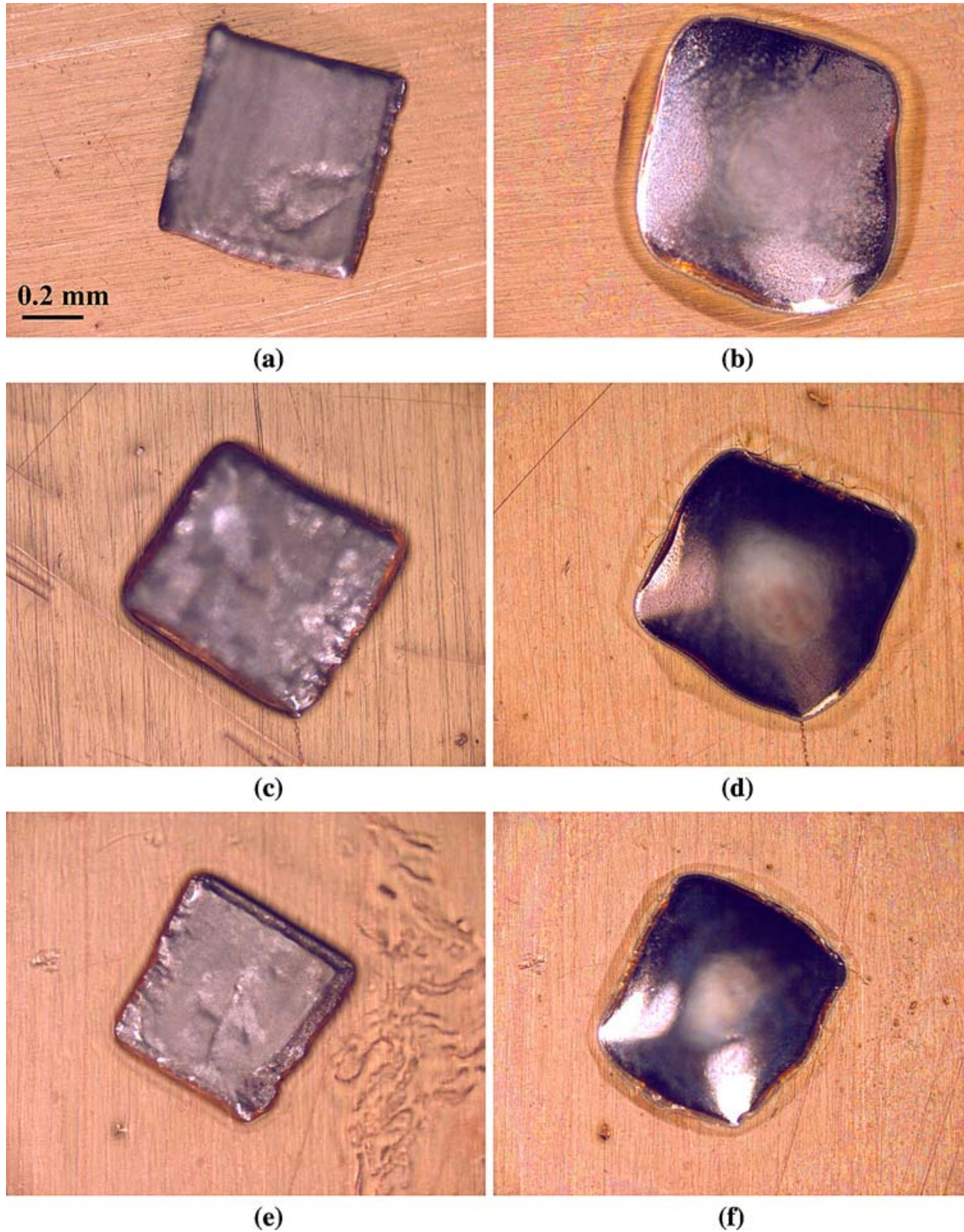

Fig. 5. Macro images of lead-free solders before and after melting (indicating only the same basic phenomenology—not for quantitative evaluation): (a, b) Sn-3.5Ag solder; (c, d) Sn solder; (e, f) Sn-0.7Cu solder.

between the liquid and solid, or σ_{LV}, the surface tension between the liquid free surface and surroundings, leads to an increase of the contact angle, hence poorer wetting.[1,15] Adding a low-surface-tension alloying element (like Pb) to Sn can reduce σ_{LV} of the alloy, and consequently may improve wetting[1,3] (the surface tension at the melting temperature for Pb, Sn, Ag, and Cu is 0.46 N/m, 0.57 N/m, 0.91 N/m, and 1.35 N/m, respectively[3]). This strategy can be pursued using a Pb-Sn solder formulation. Eutectic Pb-Sn solder has a small σ_{LV} compared with lead-free solder systems commonly used; for example, at the same temperature (250°C), tin-lead solder is characterized by σ_{LV} = 0.513 N/m (for Sn-39Pb[3]), somewhat smaller than for the corresponding surface tension of any of the considered lead-free solders, that is, σ_{LV} = 0.555 N/m for pure Sn,[3] σ_{LV} = 0.552 N/m for Sn-4Ag,[16] and σ_{LV} = 0.555 N/m for Sn-1.5Cu.[17] Hence, addition of an alloying component does not significantly change the surface tension of the lead-free solders versus pure tin. Note that the surface tension of any of these solders is larger than for the lead solder. Therefore, a certain difference in surface tension between any of the lead-free solders and the lead solder remains. So one may expect the surface tension impact of lead to be the key contributing factor to better wetting, as has been well documented in the

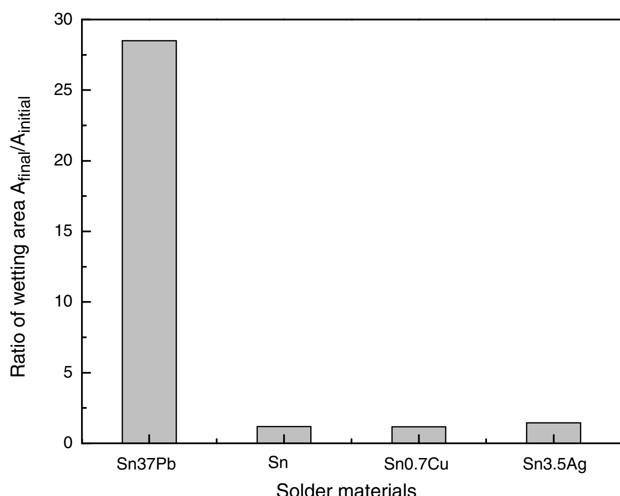

(a)

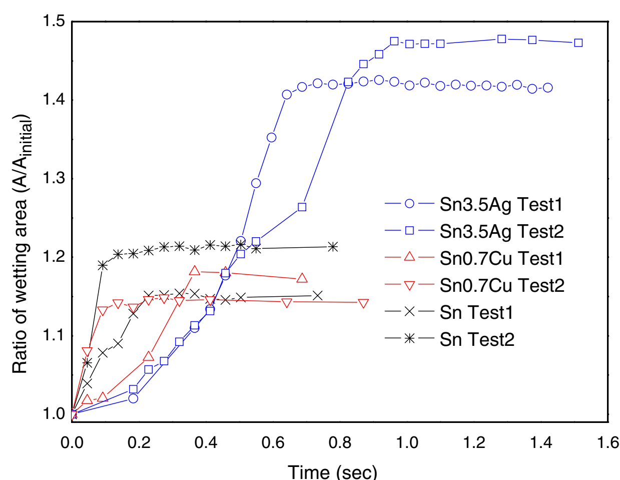

(b)

Fig. 6. A comparison of the spreading area versus initial solder area: (a) comparison of the final wetting area between lead and lead-free solders; (b) wetting kinetics of lead-free solders.

art of soldering. Still, we can hypothesize that the difference in surface tension between lead solder and any lead-free solder is not large enough to cause such an outcome; for example, if the contact angle between solder liquid with σ_{LV} = 0.555 N/m and the Cu substrate is in the range of 30 deg to 60 deg, a reduction of σ_{LV} to 0.513 N/m can lead to a less than 10 deg reduction of the contact angle. Consequently, this difference may not necessarily be the main reason for good wettability of lead solders. In other words, one should focus on the influence of interface reactions on wettability. Based on our experimental observations, the following hypothesis may be formulated: eutectic Sn-37Pb solder spreads over a Cu substrate in the presence of a reaction between Sn and Cu. Consequently, at the triple-line location a thin liquid precursor domain forms. In this domain, a large portion of Sn would be consumed by the reaction with the solid substrate, and thus Pb would

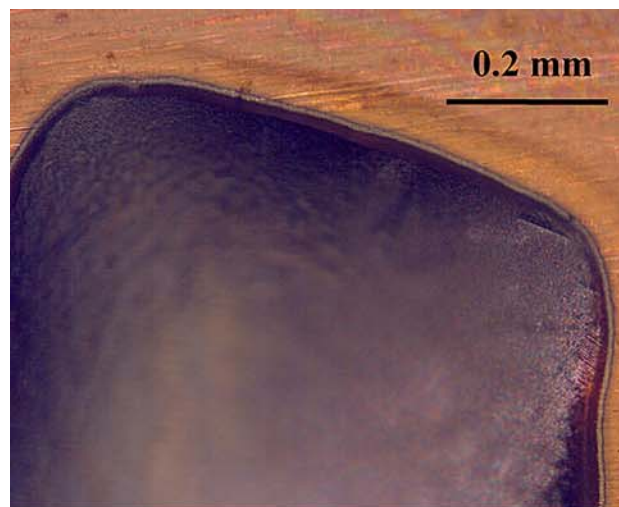

(a)

(b)

(c)

Fig. 7. Halo formation for a lead-free solder on a Cu substrate; (a) resolidified Sn-3.5Ag solder; (b) resolidified Sn solder; (c) resolidified Sn-0.7Cu solder.

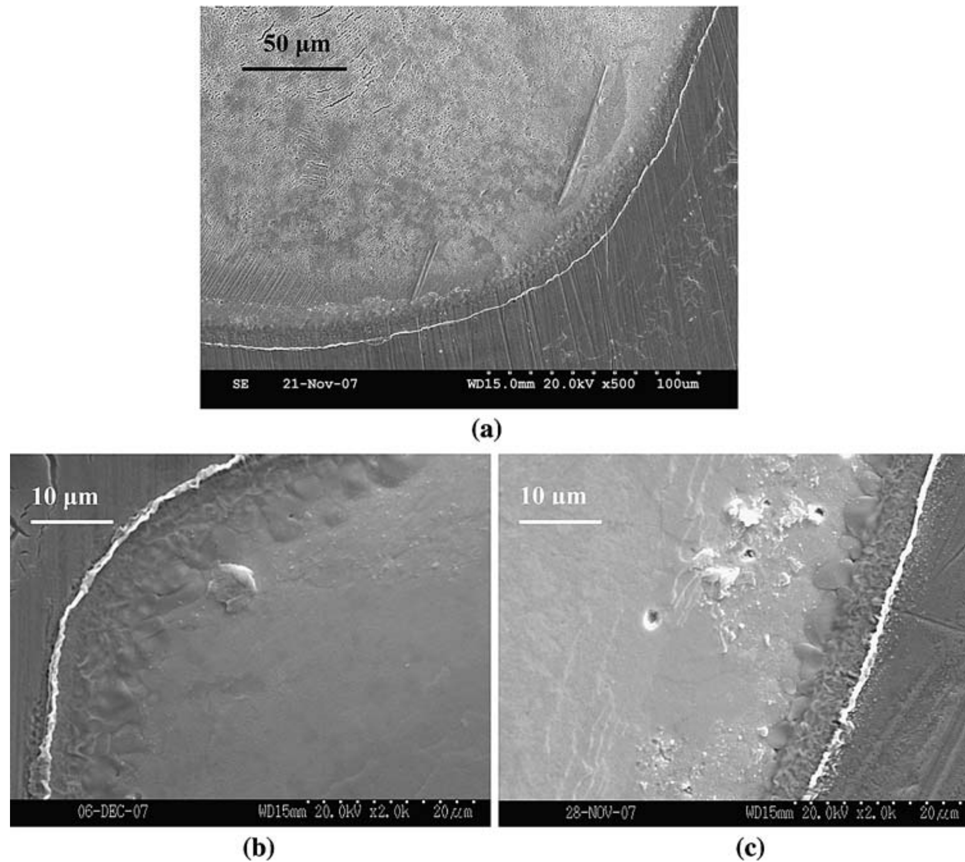

Fig. 8. SEM images of the halo region of resolidified lead-free solder; (a) Sn-3.5Ag solder; (b) Sn solder; (c) Sn-0.7Cu solder.

be increasingly left as a residue (Fig. 4b). This interface reaction and the resulting Pb residue may have two effects on promoting wetting; they may (1) reduce the surface tension between liquid and solid σ_{SL}, and (2) they may impact wetting through a change of the topography of the solid surface around the edge of the bulk liquid, i.e., they provide a network-like system of microgroove paths which may enhance the capillary effect by assisting the liquid solder to move forward. For a lead-free solder with eutectic composition, an alloying element such as Ag is added in what is comparatively a very small amount. This addition of Ag will form IMCs (Ag_3Sn) in bulk, hence further depleting the alloying component in the liquid phase. At the triple-line location a thin Sn-rich liquid precursor domain may also be observed. Therefore, the limited-size halo we observe around the bulk lead-free solder domain (Figs. 7 and 8) indicates that in that layer it was mostly Sn that was available for the reaction. The small halo region cannot additionally assist the liquid to move forward due to the lack of network-like capillary action; therefore, the lead-free solders in general offer poorer wettability.

CONCLUSIONS

The experimental wetting data trends demonstrate extensive eutectic Pb-Sn solder wetting on Cu substrates. Selected lead-free solders on a Cu substrate offer dramatically poorer wetting ability. An *in situ* observation of the solder melting and spreading processes using hot-stage microscopy provides detailed information on the triple-line movement evolution and related surface appearance of the liquid solder during spreading. Four-stage wetting kinetics was identified for eutectic Pb-Sn solder spreading on a Cu substrate. It is hypothesized that the halo formation observed in both lead and lead-free solder spreading is due to the reaction at the liquid–solid interface, i.e., the formation of the Cu_6Sn_5/Cu_3Sn intermetallic layer.

ACKNOWLEDGEMENTS

The authors acknowledge the support of the Kentucky Science and Engineering Foundation through the Grants KSEF-07-RDE-010 and KSEF-829-RDE-007. One of the authors (D.R.N.) acknowledges the support of the UK Center for Manufacturing.

REFERENCES

1. P.T. Vianco, *Soldering Handbook* (American Welding Society, 1999).
2. P.T. Vianco, Key note lecture, *3rd International Brazing and Soldering Conference*, San Antonio, Texas, April 24–26 (2006).
3. T.J. Singler, S.J. Meschter, and J. Spalik, *Handbook of Lead-Free Solder Technology for Microelectronic Assemblies*,

ed. K.J. Puttlitz and K.A. Stalter (New York, NY: Marcel Dekker, 2004).
4. Y.G. Lee and J.G. Duh, *J. Mater. Sci.* 33, 5569 (1998). doi:10.1023/A:1004499728840.
5. X.H. Wang and H. Conrad, *Scr. Metall. Mater.* 30, 725 (1994). doi:10.1016/0956-716X(94)90189-9.
6. S.J. Meschter (Ph.D. thesis, Binghamton University, 2001).
7. S.C. Kang (Ph.D. thesis, Georgia Institute of Technology, 2003).
8. H.Q. Wang, H. Zhao, D.P. Sekulic, and Y.Y. Qian, *J. Electron. Mater.* 37, 1640 (2008). doi:10.1007/s11664-008-0502-8.
9. H.Y. Chang, S.W. Chen, D.S.H. Wong, and H.F. Hsu, *J. Mater. Res.* 18, 1420 (2003). doi:10.1557/JMR.2003.0195.
10. H.Q. Wang, F.J. Wang, F. Gao, X. Ma, and Y.Y. Qian, *J. Alloys Compd.* 433, 302 (2007). doi:10.1016/j.jallcom.2006.06.076.
11. J.Q. Suh, K.N. Tu, G.V. Lutsenko, and A.M. Gusak, *Acta Mater.* 56, 1075 (2008). doi:10.1016/j.actamat.2007.11.009.
12. W.J. Boettinger, C.A. Handwerker, and L.C. Smith, *The Metal Science of Joining*, ed. M.J. Cieslsk, J.H. Perepezko, S. Kang, and M.E. Glicksman (The Minerals, Metals & Materials Society, 1992), p. 183.
13. A.M. Cazabat and M.A. Cohen Stuart, *J. Phys. Chem.* 90, 5845 (1986). doi:10.1021/j100280a075.
14. C.Y. Liu and K.N. Tu, *J. Mater. Res.* 13, 37 (1998). doi:10.1557/JMR.1998.0006.
15. P.G. De Gennes, *Rev. Mod. Phys.* 57, 827 (1985). doi:10.1103/RevModPhys.57.827.
16. J.H. Lee and D.N. Lee, *J. Electron. Mater.* 30, 1112 (2001). doi:10.1007/s11664-001-0137-5.
17. J.Y. Park, J.S. Ha, C.S. Kang, K.S. Shin, M.I. Kim, and J.P. Jung, *J. Electron. Mater.* 29, 1145 (2000). doi:10.1007/s11664-000-0005-8.